Journal of Bioenergetics and Biomembranes, Vol. 32, No. 4, 2000

Structural and Functional Features of the *Escherichia coli* F_1-ATPase

Gerhard Grüber[1]

The structural organization and overall dimensions of the *Escherichia coli* F_1-ATPase in solution has been analyzed by synchroton X-ray scattering. Using an independent *ab initio* approach, the low-resolution shape of the hydrated enzyme was determined at 3.2 nm resolution. The shape permitted unequivocal identification of the volume occupied by the $\alpha_3\beta_3\gamma$ complex of the atomic model of the ECF_1-ATPase. The position of the δ and ε subunits were found by interactive fitting of the solution scattering data and by cross-linking studies. Laser-induced covalent incorporation of 2-azido-ATP established a direct relationship between nucleotide binding affinity and the different interactions between the stalk subunits γ and ε with the three catalytic subunits (β) of the F_1-ATPase. Mutants of the ECF_1-ATPase with the introduction of Trp-for-Tyr replacement in the catalytic site of the complex made it possible to monitor the activated state for ATP synthesis (*ATP conformation*) in which the γ and ε subunits are in close proximity to the α subunits and the ADP conformation, with the stalk subunits are linked to the β subunit.

KEY WORDS: F_1-ATPase; *Escherichia coli*; small-angle X-ray scattering; quaternary structure; *ab initio* shape determination; disulfide formation.

INTRODUCTION

Adenosine 5′-triphosphate (ATP) synthesis by oxidative phosphorylation or photophosphorylation is a multistep membrane-located process that provides the bulk of cellular energy in eukaryotes and many prokaryotes. The majority of ATP synthesis is accomplished by the enzyme ATP synthase (EC 3.6.1.34)—also called F_1F_0-ATP synthase, or F_1F_0-ATPase, which, in its simplest form, as in bacteria, is composed of eight different subunits (α_3:β_3:γ:δ:ε:*a*:b_2:c_{9-12}). The latter name reflects the fact that the enzyme is reversible and can act as an ion-pumping ATPase. The F_1F_0-ATPase transforms energy from a transmembrane electrochemical gradient of ions into the phosphoric acid anhydride bond of ATP. The enzyme consists of the membrane-embedded, F_0 sector, which is involved in ion conduction, and the hydrophilic F_1 sector, including the catalytic sites for ATP synthesis and hydrolysis (Boyer, 1997; Dimroth, 1997; Weber and Senior, 1997). The later can be removed from the membrane complex *in vitro* as an active ATPase and has allowed extensive structural (Pedersen and Amzel, 1993; Walker, 1994; Capaldi *et al.*, 1996) and mechanistic studies (Junge *et al.*, 1997; Masaike *et al.*, 2000). This review describes the quaternary structure of the *Escherichia coli* F_1-ATPase in solution obtained *ab initio* from X-ray small-angle scattering data. This structure allows a comparison with structural models of F_1-ATPases determined by X-ray crystallography (Abrahams *et al.*, 1994, Shirakihara *et al.*, 1997; Bianchet *et al.*, 1998; Hausrath *et al.*, 1999). Recent work on the relationship of nucleotide binding and interac-

[1] Universität Osnabrück, Fachbereich Biologie/Chemie, Abteilung Zoophysiologie, D-49069 Osnabrück, Germany. e-mail: ggrueber@biologie.uni-osnabrueck.de

0145-479X/00/0800-0341$18.00/0

tions of stalk subunits with the major subunits α and β of the ECF_1-ATPase is then reviewed.

QUATERNARY STRUCTURE OF THE *Escherichia coli* F_1-ATPase

The fundamental aim of structural studies in molecular biology is to establish a relationship between structure (or, more precisely, structural changes) and function of biological macromolecules. Over the past years, a tremendous amount of structural information about the F_1F_0-ATPase has been obtained using macromolecular crystallography (Abrahams *et al.*, 1994, Shirakihara *et al.*, 1997; Bianchet *et al.*, 1998; Hausrath *et al.*, 1999; Stock *et al.*, 1999) and nuclear magnetic resonance (NMR) spectroscopy (Wilkens *et al.*, 1995, 1997; Girvin *et al.*, 1998; Rastogi and Girvin, 1999). Significant insights into the molecular mechanism of ATP synthesis and hydrolysis came from the X-ray structure of both the bovine heart and rat liver mitochondrial $\alpha_3\beta_3\gamma$ complex of the F_1-ATPase (Abrahams *et al.*, 1994; Bianchet *et al.*, 1998) providing a picture in which the three α and β subunits form a hexagon around a central cavity within which a part of the γ subunit is located. However, the small subunits δ and ε, as well as about one-half of the γ subunit residues, could not be resolved because of presumed disordering. Complementary to crystallographic studies, a model-independent approach, based upon the multipole expansion method by using spherical harmonics, has been used to determine the overall dimensions and the quaternary structure of the *E. coli* F_1-ATPase under nearly physiological and saturating nucleotide conditions (Svergun *et al.*, 1998a). The maximum dimension of the enzyme was found to be 15.0 ± 0.5 nm, and, as deduced both from Guinier plot and from the distance distribution function $p(r)$, its radius of gyration was 4.7 ± 0.02 nm. Its molecular mass of 390 ± 20 kDa was consistent with the value calculated from the amino acid sequence (Walker *et al.*, 1984). Qualitative analysis of the distance distribution function suggested that the ECF_1-ATPase consists of a globular core yielding a principal maximum in the $p(r)$ at $0 < r < 10$ nm with a protuberance (stalk) giving rise to a shoulder at $10 < r < 15$ nm. The shape-scattering yielded a Porod or excluded volume of the hydrated particle of 640 ± 20 nm^3, in good agreement with the molecular mass of the protein (Svergun *et al.*, 1998b).

The shape-scattering curve was used to restore the low-resolution particle shape *ab initio* at a resolution of 3.2 nm (Fig. 1). The hydrated F_1-ATPase is a compact molecule with a headpiece of approximately 10.8 nm top to bottom and 11 nm wide. However, the overall structure is asymmetric given by a stem (stalk) of approximately 4.2 nm in length and 5.3 nm in diameter. The restored envelope allowed the identification of the volume occupied by the crystallographic model of the $\alpha_3\beta_3$ subcomplex from bovine mitochondrial F_1-ATPase (Abrahams *et al.*, 1994). Its orientation along the threefold axis was uniquely selected to position the α-helical domain of the γ subunit in the protuberance of the shape (Svergun *et al.*, 1998a).

Previously, crystals containing all five subunits of ECF_1 (α_3:β_3:γ:δ:ε) and the $\alpha_3\beta_3\gamma\varepsilon$ complex have been obtained and diffracted to a resolution of 0.64 and 0.44 nm, respectively (Grüber *et al.*, 1997; Hausrath *et al.*, 1999). Besides the α and β subunits and the N- and C-terminal α helixes of the γ subunit, which showed similar features as their bovine and rat liver counterparts, the electron-density map at 0.44 nm included a number of rod-shaped features, which corresponded to additional α-helical regions within the γ subunit (Hausrath *et al.*, 1999). This structure showed that γ extended from the $\alpha_3\beta_3$ hexagon far enough to traverse the full length of the central stalk that connects the F_1 and F_0 parts (Fig. 2). Superposition of the low-resolution model of the ECF_1-ATPase with the atomic model of the ECF_1 subcomplex revealed a striking similarity, especially with respect to the disposition of the γ subunit at the bottom of the stalk (Fig. 2; Grüber, 2000). Moreover, both shapes predicted that the γ subunit will interact with the *c*-subunit ring by insertion into the dimple at the top of the ring with inner and outer dimensions of 2.5 to 3.0 nm and 5.0 to 6.2 nm, respectively (Birkenhäger *et al.*, 1995; Singh *et al.*, 1996; Rastogi and Girvin; 1999; Stock *et al.*, 1999).

ARRANGEMENT OF THE SMALLER F_1 SUBUNITS

The restored envelope allowed further analysis to be performed to determine the relative positioning of the smaller subunits δ and ε (Svergun *et al.*, 1998a). This was accomplished by the interactive three-dimensional modeling program ASSA (Kozin *et al.*, 1997) using the NMR data of the N-terminal domain of subunit δ (Wilkens *et al.*, 1997) and the ε subunit (Wilkens *et al.*, 1995; Uhlin *et al.*, 1997). The discrepancy

Fig. 1. Low-resolution model of the *E. coli* F_1-ATPase. The envelope derived from X-ray scattering data of the ECF_1-ATPase (10 mg/ml) supplemented wih 2 mM MgATP, followed by turnover of the enzyme.

between the experimental and calculated scattering curves was minimized interactively to keep the subunits within the quaternary structure of the enzyme. The solution providing the best-fit yields an *X* value of 1.68. The model indicates the δ subunit [residues 1–134 (Wilkens *et al.*, 1997)] near the bottom of the $\alpha_3\beta_3$ complex and at the interface of an αβ pair. Positioning of the δ subunit at the top of the complex correlates with higher *X* values (Svergun *et al.*, 1998a). A location of subunit δ at the bottom of an αβ interphase is in agreement with the trapped ADP conformation of the ECF_1 mutant βY331W:βE381C:εS108C (Grüber and Capaldi, 1996a) and the mutant βS383C:εS108C (Aggeler *et al.*, 1995), in which one of the intrinsic Cys residues of subunit δ interacts with the C-terminal domain at the sequence $_{380}$DCLSEED$_{386}$ of subunit β after $CuCl_2$ treatment. The fact that a disulfide bond can be formed between both subunits suggest, that one of the α-carbon atoms of the two cysteine residues (Cys64, Cys140) in the elongated δ subunit (Engelbrecht *et al.*, 1991) must be within an proximity of 4–9 Å (Creighton, 1984) to Cys381 in subunit β. By comparison, no crosslinking between Cys381 in the β and δ subunit can be obtained in the ECF_1F_0-ATP synthase (Aggeler *et al.*, 1995), implying a rearrangement of the minor subunit in the F_1-ATPase. Interestingly, an α-δ crosslink can be generated in the ECF_1-ATPase after removal of bound nucleotides (Bragg and Hou, 1986; Tozer and Dunn, 1986; Mendel-Hartvig and Capaldi, 1991; Svergun *et al.*, 1998a). However, $CuCl_2$ addition to the enzyme in the presence

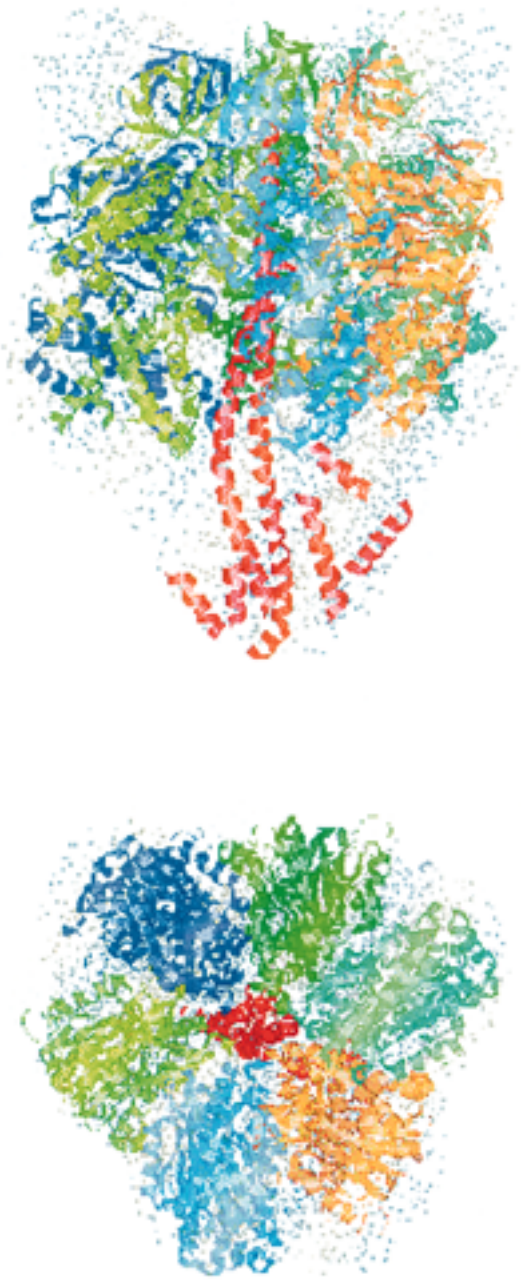

Fig. 2. A RASMOL drawing of the crystal structure of ECF_1-ATPase (Hausrath *et al.*, 1999). The structure is superimposed on an envelope of the hydrated ECF_1 complex, derived from X-ray small-angle scattering (Svergun *et al.*, 1998a) in order to compare the structural domains of both proteins. Both models were rotated counterclockwise by 90° around the *Y*- and *X*-axes.

of ATP and EDTA could not induce disulfide bond formation (Bragg and Hou, 1986), implying that the α-δ and β-δ crosslinks are made possible by flexibility

of the δ subunit in the ECF_1 complex associated with nucleotide binding. Nucleotide-dependent changes of the δ subunit have also been observed by stopped-flow fluorescence technique using N-{4-[7-(dimethylamino)-4-methyl]coumarin-3-yl}maleimide (CM) as a label (see Fig. 3). By incorporation of the fluorescent label CM into Cys140 of δ, it was shown that the fluorescence emission spectrum is sensitive to nucleotides bound in the catalytic sites. Fluorescence enhancement after the addition of MgADP and fluorescence quenching resulting from binding of MgADP and MgAMP–PNP strongly supports structural alterations in the δ subunit in response to nucleotide binding (Svergun *et al.*, 1998a).

The arrangement of the ε subunit (Wilkens *et al.*, 1995; Uhlin *et al.*, 1997) in the restored F_1 envelope involves the connections of the two helix hairpins with the $\alpha_3\beta_3$ complex and the hydrophobic side chains of the ε subunit face the γ subunit and the perpendicular face of the β-sandwich barrel (residues 31–38) is turned toward the bottom of the enzyme, as determined from the data-fitting procedure (Svergun *et al.*, 1998a). Crosslinks between the β and ε subunits induced by 1-ethyl-3-[3-(dimethylamino)propyl]carbodiimide (EDC) (Dallmann *et al.*, 1992) or disulfide bond formation between a cysteine inserted at position 381 of the β subunit and a cysteine at position 108 of the ε subunit in the presence of ADP (Aggeler *et al.*, 1995; Grüber and Capaldi, 1996a; Svergun *et al.*, 1998a) confirmed this proximity. The other major interaction of the ε subunit in ECF_1 with the γ subunit described above, has also been predicted from biochemical studies (Tang and Capaldi, 1996).

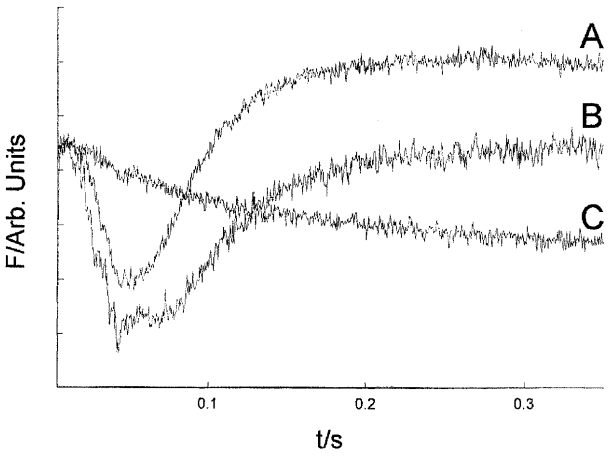

Fig. 3. Stopped-flow mixing fluorescence transient of ECF_1-ATPase labeled with CM at subunit δ (Svergun *et al.*, 1998a). The enzyme was rapidly mixed with an equal volume containing 2 mM of nucleotide (final concentration) at 12°C. The curves refer to the following nucleotides: A, MgAMP–PNP; B, MgADP; C, MgATP.

Recently, an electron density map from crystals of the $\alpha_3\beta_3\gamma\delta\varepsilon c_{10}$ subcomplex of the yeast mitochondrial ATP synthase has been obtained at 0.39=nm resolution (Stock *et al.*, 1999). Adjacent to the "bottom" part of subunit γ, the region near where γ and ε is predicted to interact with the *c*-subunit ring (Zhang and Fillingame, 1995; Capaldi *et al.*, 1996), an additional density has been observed, in which the structure of the *E. coli* ε subunit (Uhlin *et al.*, 1997), the counterpart of the yeast δ subunit (Giraud and Velours, 1994), has been modeled. This interpretation explains the interaction of the residues ε_{31-38} with the polar loops of the *c* ring (Zhang and Fillingame, 1995). However, the modeling of the *E. coli* ε subunit shows that the C-terminal α-helix is about 0.5 nm above the loops of the *c* subunits and does not, therefore, explain the close proximity of this region with the DELSEED region of a β subunit, which is believed to be involved in the coupling of catalytic site events (Capaldi *et al.*, 1996) along with γ and ε acting as a rotor (Schulenberg *et al.*, 1997; Bulygin *et al.*, 1998; Kato-Yamada *et al.*, 1998; Aggeler *et al.*, 1997). This discrepancy could be due, at least in part, to the dissociation of the complex during crystallization and could therefore account for a rearrangement of the yeast δ subunit, that has a sequence identity of only 21% to the *E. coli* ε subunit (Giraud and Velours, 1994).

INTERACTION OF THE γ AND ε WITH THE CORE $\alpha_3\beta_3$ COMPLEX DURING COUPLING

X-ray structure analysis of the F_1-ATPase (Abrahams *et al.*, 1994; Shirakihara *et al.*, 1997; Bianchet *et al.*, 1998) suggest that the three catalytic sites of the complex are located at the interfaces between the α and β subunits, with the large majority of protein-to-nucleotide ligands provided by the β subunit. The three sites have different conformations and nucleotide contents, one of which contains the ATP homolog AMP–PNP, the second ADP, and the third is distorted and empty (Abrahams *et al.*, 1994). In addition to the three catalytic sites, the F_1-ATPase contains three noncatalytic sites at the α subunits that bind MgATP, but do not hydrolyze it. The ECF_1-ATPase binds MgATP under stoichiometric amounts at the first site (single-site) with high affinity ($K_d \approx 10^{-9}$ M; Weber *et al.*, 1993; Grüber and Capaldi, 1996a) and hydro-

lyzes the substrate slowly in what is called *unisite catalysis*. Occupation of the second and third site by MgATP, which occurs with significantly lower affinity (negative cooperativity), induces an overall positive catalytic cooperativity (Cross, 1988). The structural and binding data raise the obvious question, what determines the states of the different catalytic sites?

To investigate this question, ECF_1-ATPase from the mutant βE381C:εS108C was treated with different concentrations of [^{3}H]-2-azido-ATP and covalent insertion of the nucleotide analog induced by photoactivation of the azide group with single-pulse UV laser excitation (Grüber and Capaldi, 1996a). The enzyme showed cooperative binding of [^{3}H]-2-azido-ATP in the presence of Mg^{2+}. The highest affinity site ($K_d \approx$ 100 nM) was located at β_{free}, the one of the three β subunits in the mutant that does not form $CuCl_2$-induced disulfide bonds with either the γ or the ε subunit. This β subunit was, therefore, the site of unisite catalysis in the enzyme. The second [^{3}H]-2-azido-ATP binding site ($K_d \approx 1–2$ μM) was located in the β subunit that links to ε (β_ε), whereas the lowest affinity binding site ($K_d \approx 20–30$ μ*M*) was in the β subunit that links to γ(β_γ).

In parallel, two new mutants were created (Grüber and Capaldi, 1996a), one a double mutant (βY331W:βE381C) containing the introduced Cys residue in β and the Trp-for-Tyr exchange in the catalytic site, by which it was possible to directly monitor nucleotide binding in catalytic sites. The second, a triple mutant, contained βY331W:βE381C plus the mutation εS108C. The potential importance of the triple mutant was that, by inducing a disulfide bond, a quantitative crosslink between one β and γ (via βE381C and γCys87) and β and ε (via βE381C and εS108C) could be formed, which facilitated the clear differentiation between the three subunits (β_{free}, β_γ, β_ε). When 20 μM $CuCl_2$ was present with the triple mutant, only a β-ε disulfide bond could be made selectively. With the double mutant (βY331W:βE81C) a third enzyme conformation, β-γ could be created.

As observed by fluorescence studies, binding of MgATP to the βY331W:βE381C:εS108C mutant quenched the fluorescence of the introduced Trp residues, resulting in a fluorescence spectrum similar to that of wild-type enzyme. Titration revealed binding of three moles of ATP per mole of ECF_1 with three different dissociation constants (K_d) of 90 nM, 2 μM, and 40 μM, values close to those recorded in the [^{3}H]-2-azido-ATP experiments. Formation of S-S bridges between β-ε or β-ε and β-γ had very little effect on nucleotide binding. The binding affinities of the three catalytic sites for MgATP were not significantly altered from those obtained before crosslinking and the enzyme continued to switch between cooperative binding (Grüber and Capaldi, 1996a).

By analogy to the βY331W:βE381C:εS108C mutant, a third mutant (αS411C:βY331W:εS108C) has been generated with a Cys residue in αS411C, which is equivalent to Glu_{381} in the DELSEED region of the β subunit (Grüber and Capaldi, 1996b). When the γ and ε subunits were crosslinked to α subunits, ATP binding in the highest affinity catalytic site was dramatically altered. This site became closed so that nucleotide that had been bound into it prior to crosslinking was trapped and could not be exchanged. In addition, ATP or ADP could not enter this site. Finally, crosslinking of the γ and ε to the α subunits disabled the switching between cooperative binding. The combination of results from these different mutants suggests that the conformation of the enzyme in which the small subunits are at α subunits occurs during function of the enzyme in the course of the movement(s) of γ and ε subunits within the $\alpha_3\beta_3$ hexamer and that this may be the activated state for ATP synthesis.

The structural parameters and the shape of the hydrated ECF_1-ATPase determined by small-angle X-ray scattering together with the superposition of the $\alpha_3\beta_3\gamma$ complex of the same enzyme give a well-defined description of the structural features of this complex. $CuCl_2$-induced cross-link fomation between various subunits of the ECF_1-ATPase have contributed significantly to our understanding of the subunit–subunit interactions of the enzyme as a function of nucleotide binding. The key to understanding the overall mechanism of coupling within the F_1F_0-ATP synthase is to characterize the structural changes in the F_0 portion, due to ion translocation, that are linked to conformational changes in γ and ε subunits. Ultimately, it will be likely to be necessary to have a high-resolution structure of the complete F_0 portion to fully appreciate the mechanism of conformational coupling in this enzyme.

ACKNOWLEDGMENTS

The author is supported by a Habilitandenstipendium (GR 1475/6-1) of the Deutsche Forschungsgemeinschaft (DFG).

REFERENCES

Abrahams, J. P., Leslie, A. G. W., Lutter, R., and Walker, J. E. (1994). *Nature (London)* **370**, 621–628.

Aggeler, R., Haughton, M. A., and Capaldi, R. A. (1995). *J. Biol. Chem.* **270**, 9185–9191.

Aggeler R., Ogilvie I., and Capaldi R. A. (1997). *J. Biol. Chem.* **272**, 19621–19624.

Bianchet, M. A, Hullihen, J. Pedersen, P. L., and Amzel, M. L. (1998). *Proc. Natl. Acad. Sci. USA* **95**, 11065–11070.

Birkenhäger, R. Hoppert, M., Deckers-Hebestreit, G., Mayer, F., and Altendorf, K. (1995). *Eur. J. Biochem.* **230**, 58–67.

Boyer, P. D. (1997). *Annu. Rev. Biochem.* **66**, 717–749.

Bragg, P.D. and Hou, C. (1986). *Biochim. Biophys. Acta.* **851**, 385–394

Bulygin, V. V., Duncan, T. M., and Cross, R. L. (1998). *J. Biol. Chem.* **273**, 31765–31769.

Capaldi, R. A., Aggeler, R., Wilkens, S., and Grüber, G. (1996). *J. Bioenerg. Biomembr.* **28**, 397–401.

Creighton, T. E. (1984). *Methods Enzymol.* **107**, 305–329.

Cross, R. L. (1988). *J. Bioener. Biomembr.* **20**, 395–405.

Dallmann, H. G., Flynn, T.G., and Dunn, S.D. (1992). *J. Biol. Chem.* **270**, 24609–24614.

Dimroth, P. (1997). *Biochim. Biophys. Acta* **1318**, 11–51.

Engelbrecht, S., Reed, J., Pennin, F., Gautheron, C., and Junge, W. (1991). *Z. Naturforsch.* **46c**, 759–764.

Giraud, M.-F. and Velours, J. (1994). *Eur. J. Biochem.* **222**, 851–859.

Girvin, M. E., Rastogi, V. K., Abildgaard, F., Markley, J. L., and Fillingame, R. H. (1998). *Biochemistry* **37**, 8817–8824.

Grüber, G. (2000). *Habilitationthesis*, University of Osnabrück.

Grüber, G. and Capaldi, R. A. (1996a). *Biochemistry* **35**, 3875–3879.

Grüber, G. and Capaldi, R. A. (1996b). *J. Biol. Chem.* **271**, 32623–32628.

Grüber, G., Hausrath, A. C., Sagermann, M., and Capaldi, R. A. (1987). *FEBS Lett.* **410**, 165–168.

Hausrath, A. C., Grüber, G., Matthews, B. W., and Capaldi, R. A. (1999). *Proc. Natl. Acad. Sci. USA* **96**, 13697–13702.

Junge, W., Lill, H., and Engelbrecht, S. (1997). *Trends Biochem. Sci.* **22**, 420–423.

Kato-Yamada, Y., Noji, H., Yasuda, R., Kinosita, K. Jr., and Yoshida, M. (1998). *J. Biol. Chem.* **273**, 19375–19377.

Kozin, M. B, Volkov, V. V., and Svergun, D. I. (1997). *J. Appl. Crystallogr.* **30**, 811–815.

Masaike, T., Mitome, N., Noji, H., Muneyuki, E., Yasuda, R., Kinosita, J. Jr., and Yoshida, M. (2000). *J. Exp. Biol.* **203**, 1–8.

Mendel-Harting, J. and Capaldi, R. A. (1991). *Biochim. Biophys. Acta.* **1060**, 115–125.

Pedersen, P. L. and Amzel, M. (1993). *J. Biol. Chem.* **268**, 9937–9940.

Rastogi, V. K. and Girvin, M. E. (1999). *Nature (London)* **402**, 263–268.

Schulenberg, B., Wellmer, F., Lill, H., Junge, W., and Engelbrecht, S. (1997). *Eur. J. Biochem.* **249**, 131–141.

Shirakihara, Y., Leslie, A. G. W., Abrahams, J. P., Walker, J. E., Ueda, T., Sekimoto, Y., Kambara, M., Saika, K., Kagawa, Y., and Yoshida, M. (1997). *Structure* **5**, 825–836.

Singh, S., Turina, P., Bustamante, C. J., Keller, D. J., and Capaldi, R. A. (1996). *FEBS Lett.* **397**, 30–34.

Stock, D., Leslie, A. G. W., and Walker, J. E. (1999). *Science* **286**, 1700–1705.

Svergun, D. I., Aldag, I., Sieck, T., Altendorf, K., Koch, M. H. J., Kane, D., Kozin, M. B., and Grüber, G. (1998a). *Biophys. J.* **75**, 2212–2219.

Svergun, D. I., Konrad, S., Huss, M., Koch, M. H. J., Wieczorek, H., Altendorf, K., Volkov, V. V., and Grüber, G. (1998b). *Biochemistry* **37**, 17659–17663.

Tang, C. and Capaldi, R. A. (1996). *J. Biol. Chem.* **271**, 3018–3024.

Tozer, R. G. and Dunn, S. D. (1986). *Eur. J. Biochem.* **161**, 513–518.

Uhlin, U., Cox, G. B., and Guss, J. M. (1997). *Structure* **5**, 1219–1230.

Walker, J. E. (1994). *Curr. Opinion Struct. Bio.* **4**, 912–918.

Walker, J. E., Saraste, M, and Gay, N. J. (1984). *Biochim. Biophys. Acta* **768**, 164–200.

Weber, J. and Senior, A. E. (1997). *Biochim. Biophys. Acta* **1319**, 19–58.

Weber, J., Wilke-Mounts, S., Lee, R. S. F., Grell, E., and Senior, A. E. (1993). *J. Biol. Chem.* **268**, 20126–20133.

Wilkens, S., Dahlquist, F. W., McIntosh, L. P., Donaldson, L. W., and Capaldi, R. A. (1995). *Nature Struct. Biol.* **2**, 961–967.

Wilkens, S., Dunn, S. D., Chandler, J., Dahlquist, F. W., and Capaldi, R. A. (1997). *Nature Struct. Biol.* **4**, 198–201.

Zhang, Y. and Fillingame, R. H. (1995). *J. Biol. Chem.* **270**, 24609–24614.